Supporting Information

High-Efficient Electrocatalyst for Overall Water Splitting: Mesoporous CoS/MoS_2 with Hetero-Interface

Wen-Huan Huang,[*ab] *Xi-Ming Li,*[a] *Xiu-Fang Yang,*[a] *Hua-Bin Zhang,*[c] *Fei Wang,*[b] *and Jian Zhang,*[*b]

[a] Key Laboratory of Chemical Additives for China National Light Industry, College of Chemistry and Chemical Engineering, Shaanxi University of Science and Technology, 710021, Xi'an, China

[b] State Key Laboratory of Structural Chemistry, Fujian Institute of Research on the Structure of Matter, Chinese Academy of Sciences, 350002, Fuzhou, China

[c] KAUST Catalysis Center, King Abdullah University of Science and Technology, 23955-6900, Thuwal, Kingdom of Saudi Arabia

1. EXPERIMENTAL SECTION

1.1 Materials.

Co-balt(II) acetate tetrahydrate (99.5%), 2-Ethylimidazole (99%), Molybdic(VI) acid (99%), Polyvinylpyrrolidone (K30), Thioacetamide (99%), Nafion solution (5 wt%). All chemicals were commercial sources and used as received without any further purification.

1.2 Synthesis of HZIF-1-CoMo.

A mixture of 2-ethylimidazole (2.3 g, 24 mmol), $Co(CH_3COO)_2 \cdot 4H_2O$ (3.98 g, 16 mmol), H_2MoO_4 (0.640 g, 4 mmol) and DMF (150ml) were vigorously stirred for about 30 minutes and then heated at 160 ^oC for 1 day. The resultant bluish violet HZIF-1-CoMo crystals were formed and filtered out, washed with fresh DMF and methanol (1:1, 50 mL) and then dried in air with the yield of 73%.

1.3 Synthesis of CoS/MoS_2 polyhedron.

Fifty milligrams of HZIF-1-CoMo crystals were dispersed in 120 mL of ethanol under ultrasonic treatment for 30 min, forming a uniform solution A. Then, the thioacetamide (3.75 mM) was dispersed in 40 mL of ethanol as solution B. These two solutions were mixed and kept stirring at 90 °C for 1 hour. The black product of CoS/MoS_2 was obtained by several rinsing-centrifugation cycles with deionized (DI) water/ ethanol (1:1, 40mL) solution and then dried at 50 °C.

1.4 Synthesis of CoS.

A mixture of Cobalt nitrate hexahydrate (0.722 g), 2-Methylimidazole (1.629 g) and DMF (50ml) were mixed and vigorously stirred for about 3 minutes. The mixture solutions were kept at room temperature for 24 h. The resultant bluish violet ZIF-67 particles were obtained by several rinsing-centrifugation cycles with methanol and then dried at 60 °C overnight. 50 mg of ZIF-67 particles were dispersed in 120 mL of ethanol under ultrasonic treatment for 30 min, forming a uniform solution A. Then, the thioacetamide (3.75 mM) was dispersed in 40 mL of ethanol as solution B. These two solutions were mixed and kept stirring at 90 °C for 1 hour. The black product of CoS was obtained by several rinsing-centrifugation cycles with deionized (DI) water/ ethanol (1:1, 40mL) solution and then dried at 50 °C.

1.5 Synthesis of MoS_2.

The preparation process of MoS_2 is as follows: Fifty milligrams of $Na_2MoO_4·2H_2O$ was dissolved in 20 mL of Milli-Q water, forming a homogeneous solution A. Then, Fifty milligrams of CH_3CSNH_2 was dissolved in 20 mL of ethanol as solution B. Whereafter, the solution A was slowly added into the solution B, followed by ultrasonic treatment for 30 min. Afterward, the mixture was transferred to the Teflon-lined stainless-steel autoclave (50 mL) and heated at 200 °C for 12 h. The precipitate of MoS_2 was obtained by several rinsing-centrifugation cycles with ethanol and then dried at 60 °C for 12 h.

2.1 Characterization.

The powder X-ray diffraction (PXRD) patterns were measured on an D8 DAVANCI X-ray powder diffractometer with Cu Kα radiation ($\lambda = 0.1542$ nm). Scanning electron microscopy (SEM) results were captured by the Hitachi S4800 (2 kV). Thermogravimetry analysis (TGA) were tested by a thermogravimetric analyzer (TA Q50) under an N_2 atmosphere with the heating rate of 5 ^{o}C/min. The Brunauer-Emmett-Teller (BET) specific surface area was evaluated using N_2 adsorption–desorption on an ASAP 2020 sorption system by N_2 adsorption and desorption curves at 77K. The compounds were pressed into pellets with KBr for the Fourier transformed-infrared (FT-IR) study on the Bruker TENSOR 27 in the region of 400-4000 cm^{-1}. Transmission electron microscopy (TEM), high-resolution transmission electron microscopy (HRTEM) and elemental mapping were recorded on JEM-2010HR apparatus (200kV). X-ray photoelectron spectroscopy (XPS) spectra of the product were recorded on a Thermo ESCA Lab250XI. Raman spectra were obtained on a Labram HR800 Evolution spectrometer system using 633 nm.

2.2 Electrochemical Measurement.

Electrochemical experiments were carried out on CHI 660E electrochemical station (Shanghai Chenhua Co., China) in a typical three-electrode system at room temperature. The catalysts coated on glassy carbon electrode (GCE) with diameter of 3 mm, the Ag/AgCl electrode (3.0 M KCl), and the platinum electrode were used as the working, reference and counter electrode for OER electrocatalysis. For HER electrochemical experiments, the carbon rod electrode was used as counter electrode compared to OER. The current density was normalized to the geometrical surface area (0.07 cm^2). All potentials were calculated with respect to reversible hydrogen electrode (RHE) based on: E (RHE) = E vs. (Ag/AgCl) + 0.059pH + 0.197 V. The overpotential (η) was calculated by η (V) = E (RHE) - 1.23 V for OER. In addition, the overpotential (η) was calculated by η (V) = 0 V - E (RHE) for HER. Tafel slope was calculated from the following equation, η = b log(j)+ a, where η is the overpotential, j is the current density, and b is the Tafel slope.

Before each test, the working electrode was fabricated as follows. 5.0 mg grinded CoS/MoS_2 electrocatalysts and 0.03 mL Nafion solution (5.0 wt%) were added in 0.97 mL ethanol, and further dispersed by 20 min sonication into homogeneous suspension. Then, 5.5 μL suspension was pipetted onto glassy carbon electrode, which was mechanically polished and ultrasonically washed in advance. Ultimately, the working electrode was prepared after solvent evaporation in air for 5.0 min. The preparation of the working electrode for overall water splitting was fabricated as follows: 1cm×2cm×1mm nickel foam (NF) was cleaned by ultrasound in 0.1M H_2SO_4, anhydrous ethanol and distilled water, respectively, for three times, and then dried in vacuum oven. Above synthesized CoS/MoS_2 suspension was dropped on the NF with the loading amount of 2 mg cm^{-2}, and vacuum-dried as the working electrode.

OER tests: Before each test, 1 M KOH solution was bubbled for about 10 minutes to saturate it. Linear sweep voltammetry (LSV) was tested at a scan rate of 2 mV s^{-1} from 1.0 to 1.6 V *vs.* RHE in alkaline media. The iR compensation (correction of the voltage drop caused by resistance) was based on the positive feedback method, and the compensation level is 100%. The electrochemical double layer capacitance (C_{dl}) was investigated by cyclic voltammograms at various scanning rates (10, 20, 30, 40, 50 and 60 mV/s) in a narrow potential range of 1.19 to 1.29 V *vs.* RHE in alkaline media, respectively. The C_{dl} values can be obtained from the fitting line of the current density versus scan rate plot. The electrochemical impedance spectrum (EIS) was collected by applying an AC voltage with 5 mV amplitude in a frequency range from 100,000 to 0.1 Hz. The chronopotentiometry was conducted at the current density of 10 mA cm^{-2}.

HER tests: LSV was tested with a scan rate of 2 mV s^{-1} from -1.0 to -1.8 V *vs.* Ag/AgCl in alkaline media. The cyclic voltammograms was conducted at the range from -0.9 to -1.0 V *vs.* Ag/AgCl. The iR compensation, C_{dl}, EIS, and i-t scanning was collected at the same methods with the OER tests.

Electrocatalytic overall water splitting: The symmetric full electrolyzer was assembled by using CoS/MoS_2 loaded NFs (loading amount of 2 $mg \cdot cm^{-2}$) as both cathode and anode in 1 M KOH solution. LSV was tested at a scan rate of 2 mV s^{-1} from 1.0 to 1.9 V.

2. SUPPORTING FIGURES AND TABLES

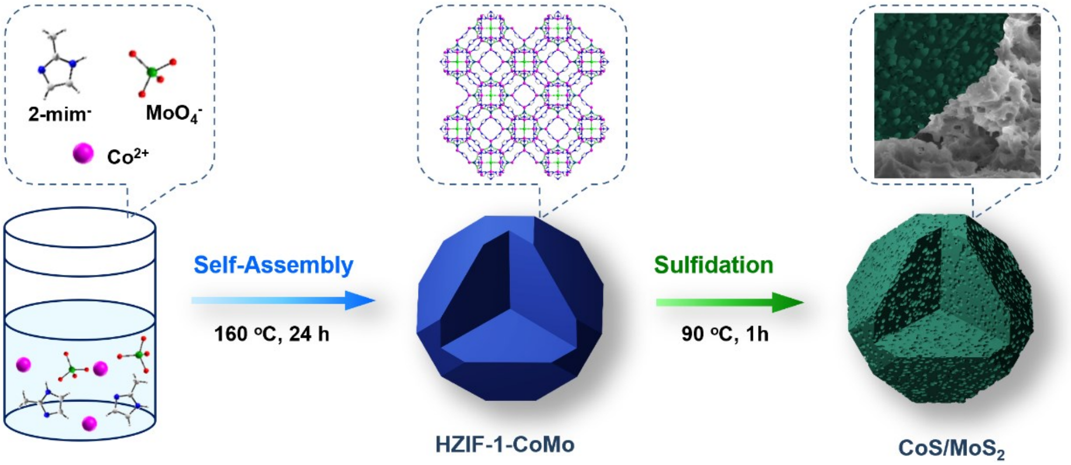

Figure S1. Illustration of the fabrication process of the mesoporous CoS/MoS_2 polyhedrons.

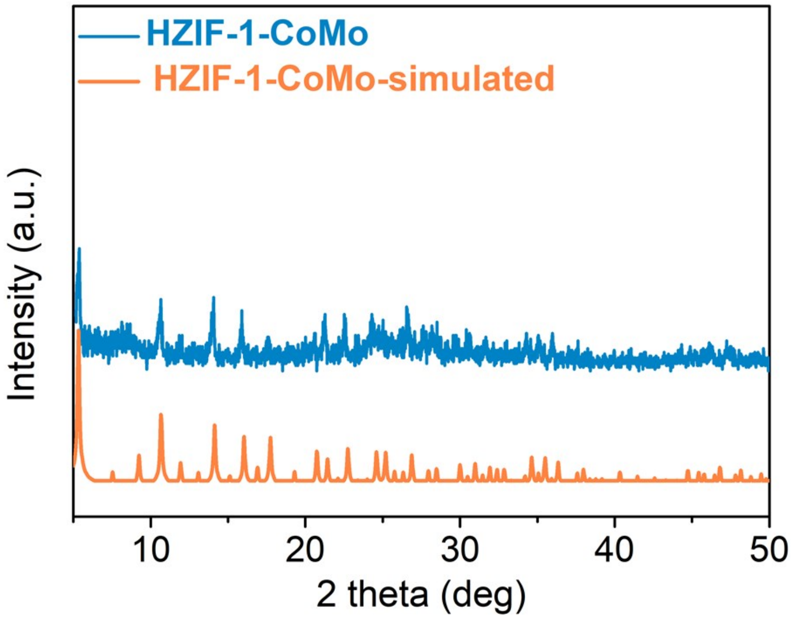

Figure S2. XRD patterns of HZIF-1-CoMo

The thermal stabilities of HZIF-1-CoMo and CoS/MoS_2 are studied by TGA analysis under N_2 atmosphere. The combining inorganic MoO_4 units into the crystalline structure endows HZIF-1-CoMo with great thermal stability before 500 ^{o}C. The mesoporous CoS/MoS_2 displays a fast collapse after being heated, indicating its poor thermal stability (Fig. S3).

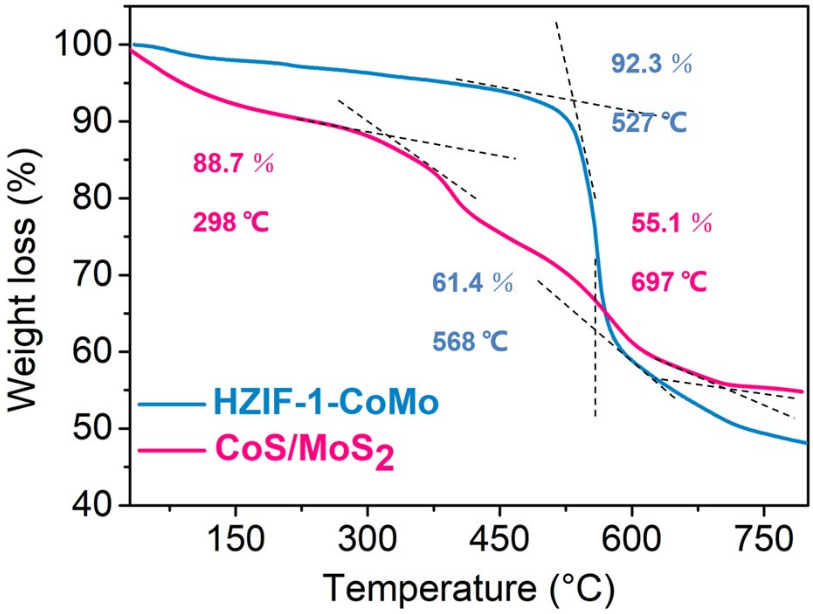

Figure S3. TGA results (under N_2 atmosphere) of HZIF-1-CoMo and CoS/$MoS_{2.}$

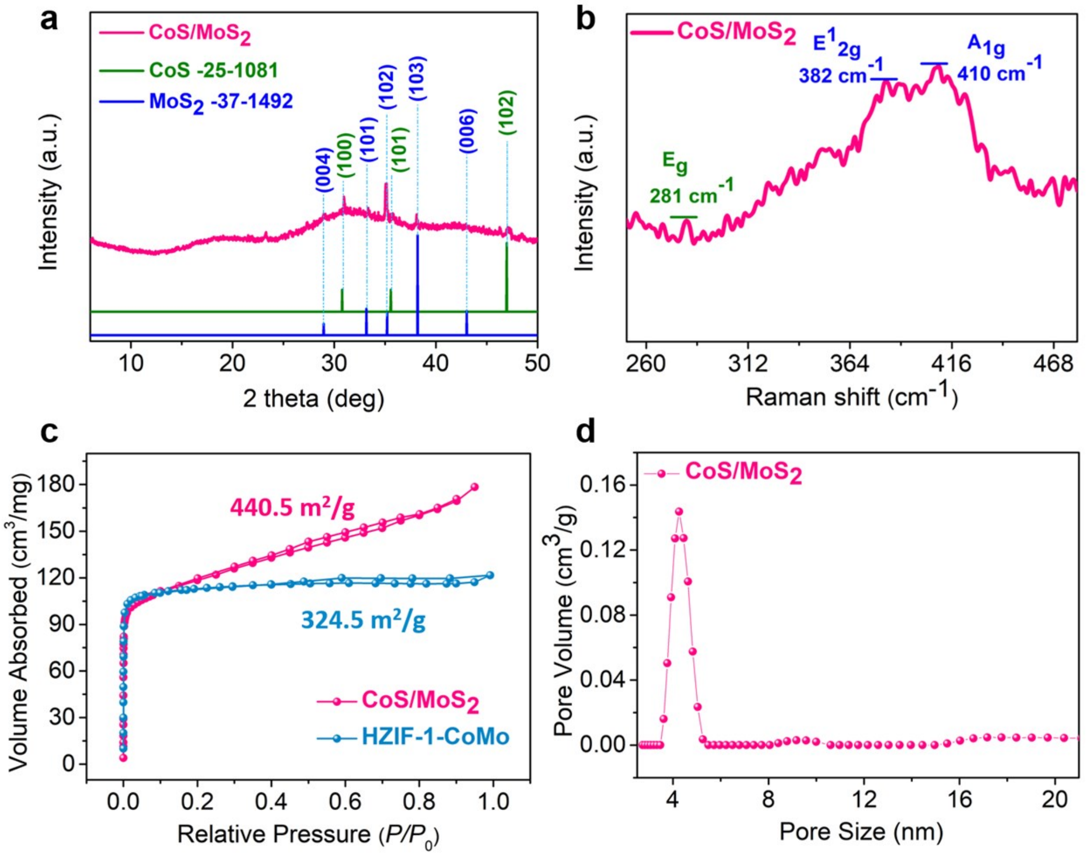

Figure S4. XRD patterns of CoS/MoS_2 (a), Raman curve of CoS/MoS_2 (b), Nitrogen adsorption-desorption isotherm curves of HZIF-1-CoMo and CoS/MoS_2 (c), Pore size distribution of CoS/MoS_2 (d).

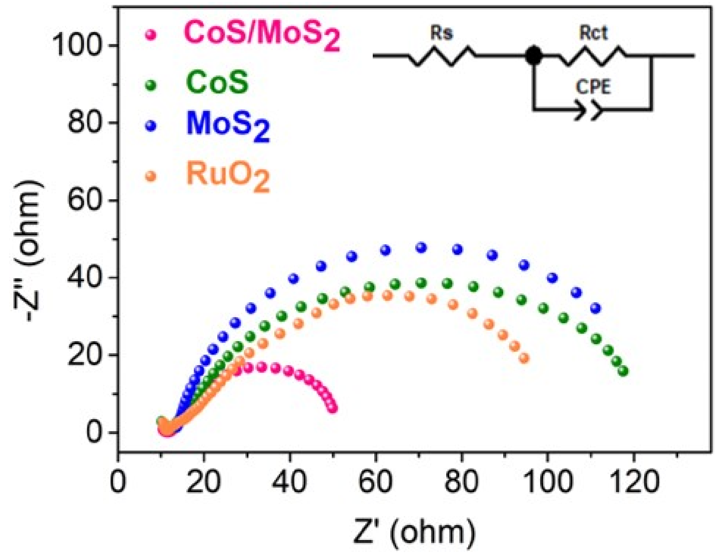

Figure S5. EIS results of CoS/MoS_2, CoS, MoS_2 and RuO_2 for electrocatalytic oxygen evolution reaction in 1M KOH

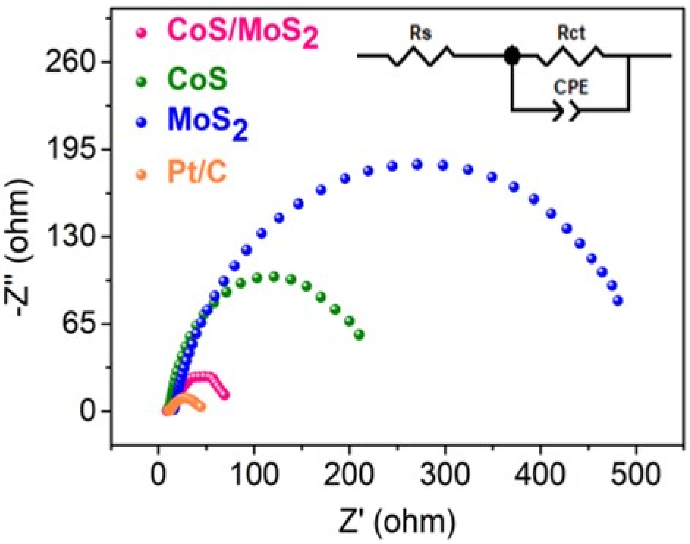

Figure S6. EIS results of CoS/MoS_2, CoS, MoS_2 and Pt/C (20 wt%) for electrocatalytic hydrogen evolution reaction in 1M KOH

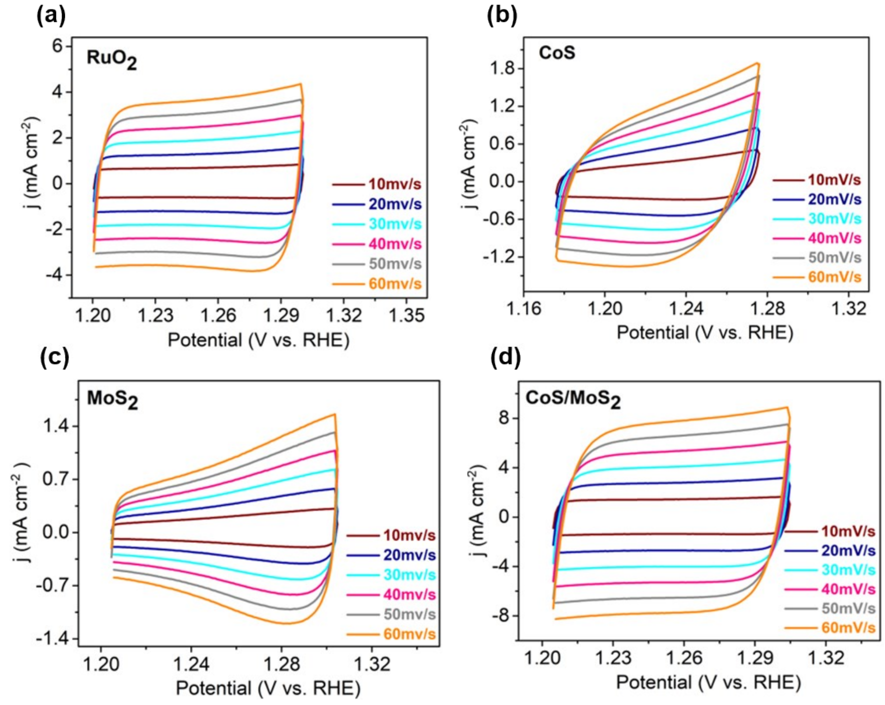

Figure S7. Cyclic voltammograms in the double-layer region of the electrodes loaded with (a) RuO_2, (b) CoS, (c) MoS_2 and CoS/MoS_2 in oxygen evolution reaction electrocatalysis.

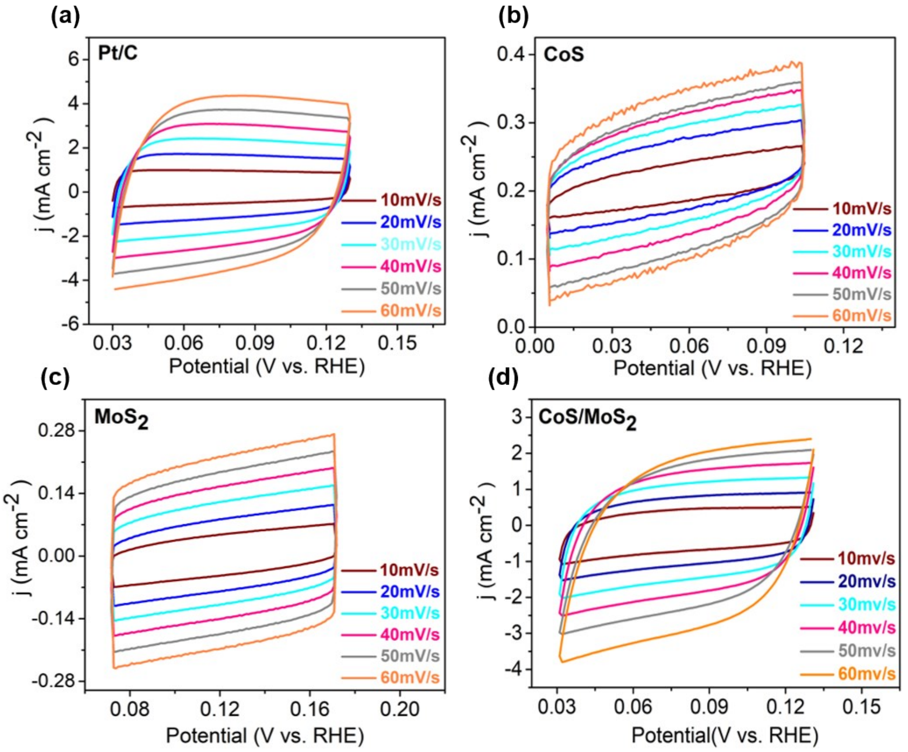

Figure S8. Cyclic voltammograms in the double-layer region of the electrodes loaded with (a) Pt/C (20 wt%), (b) CoS, (c) MoS_2 and CoS/MoS_2 in hydrogen evolution reaction electrocatalysis.

Table S1. Summary the data of the electrochemically active surface area for OER electrocatalysis in 1M KOH.

Catalyst	C_{dl} (mF cm^2)	Cs (mF)	ECSA (cm^2)
CoS/MoS$_2$	87	0.85	102.35
CoS	7	0.85	8.24
MoS$_2$	5	0.85	5.88
RuO$_2$	14	0.85	16.47

Table S2. Summary the data of the electrochemically active surface area for HER electrocatalysis in 1M KOH.

Catalyst	C_{dl} (mF cm^2)	Cs (mF)	ECSA (cm^2)
CoS/MoS$_2$	35.1	0.85	41.29
CoS	1.8	0.85	2.12
MoS$_2$	0.8	0.85	0.94
Pt/C	67.9	0.85	79.88

Table S3. Comparison of electrochemical parameters of CoS/MoS$_2$ and other reported Overall Water Splitting catalysts in 1M KOH.

Catalysts	HER Potential vs. RHE(V)@10 mA cm^{-2}	OER Potential vs. RHE(V)@10 mA cm^{-2}	Overall Water Splitting Potential (V) @10 mA cm^{-2}	Reference
CoS/MoS$_2$	-0.180	1.511	1.61	This work
CoP/NCNHP	-0.115	1.54	1.64	J. Am. Chem. Soc. 2018, 140, 2610-2618.
Co/W-C@NCNSs	-0.252	1.553	1.68	Energy Technology, 2019,1.
Co-NCNTFs//NF	-0.141	1.46	1.62	ACS Appl. Mater. Interfaces, 2020, 12(3): 3592-3602.

MoS_2@CoNi-ZIF(3-1)	-0.153	1.47	1.55	Appl. Catal. B-Environ, 2019.7,117970.
Mo_2C@CS	-0.06	1.55	1.73	ChemSusChem, 2017, 10, 3540.
CoP/rGO	-0.15	1.57	1.7	Chem. Sci., 2016, 7, 1690.
$NiCo_2O_4$	-0.19	1.5	1.65	Angew. Chem. Int. Ed., 2016, 55, 6290.
Co-Pt/C NAs	-0.05	1.55	1.54	J. Mater. Chem. A, 2018,9.
Co-S sheets	-0.19	1.536	1.743	ACS Nano, 2016, 10, 2342.
ZnCoS-NSCNT/NP	-0.152	1.50	1.59	J. Mater. Chem. A, 2018, 6, 10441.

3. REFERENCES

(1) Pan, Y.; Sun, K. A.; Liu, S. J.; Cao, X.; Wu, K. L.; Cheong, W.-C.; Chen, Z.; Wang, Y.; Li, Y.; Liu, Y. Q.; Wang, D. S.; Peng, Q.; Chen, C.; Li, Y. D. Core–Shell ZIF-8@ZIF-67-Derived CoP Nanoparticle-Embedded N-Doped Carbon Nanotube Hollow Polyhedron for Efficient Overall Water Splitting. *Journal of the American Chemical Society.* **2018,** 140, 2610-2618.

(2) Zhao, T.; Gao, J. K.; Wu, J.; He, P. P.; Li, Y. W.; Yao, J. M. Highly Active Cobalt/Tungsten Carbide-Doped Porous Carbon Nanomaterials Derived from Metal-Organic Frameworks as Bifunctional Catalysts for Overall Water Splitting. *Energy Technol.* **2019,** 7.

(3) Yuan, Q. Y.; Yu, Y. X.; Gong, Y. J.; Bi, X. F. Three-Dimensional N-Doped Carbon Nanotube Frameworks on Ni Foam Derived from a Metal-Organic Framework as a Bifunctional Electrocatalyst for Overall Water Splitting. *ACS Appl Mater Interfaces.* **2020,** 12, 3592-3602.

(4) Liu, Y. K.; Hu, B.; Wu, S. D.; Wang, M. H.; Zhang, Z. H.; Cui, B. B.; He, L. H.; Du, M. Hierarchical nanocomposite electrocatalyst of bimetallic zeolitic imidazolate framework and MoS_2 sheets for non-Pt methanol oxidation and water splitting. *Applied Catalysis B: Environmental.* **2019,** 258.

(5) Wang, H.; Cao, Y. J.; Sun, C.; Zou, G. F.; Huang, J. W.; Kuai, X. X.; Zhao, J. Q.; Gao, L. J. Strongly Coupled Molybdenum Carbide on Carbon Sheets as a Bifunctional Electrocatalyst for Overall Water Splitting. *ChemSusChem.* **2017,** 10, 3540-3546.

(6) Jiao, L.; Zhou, Y.-X.; Jiang, H.-L. Metal-organic framework-based CoP/reduced graphene oxide: high-performance bifunctional electrocatalyst for overall water splitting. *Chem. Sci.* **2016,** 7, 1690-1695.

(7) Gao, X. H.; Zhang, H. X.; Li, Q. G.; Yu, X. G.; Hong, Z. L.; Zhang, X. W.; Liang, C. D.; Lin, Z. Hierarchical $NiCo_2O_4$ Hollow Microcuboids as Bifunctional Electrocatalysts for Overall Water-Splitting. *Angew. Chem., Int. Ed.* **2016,** 55, 6290-6294.

(8) Zhang, H.; Liu, Y. Y.; Wu, H. J.; Zhou, W.; Kou, Z. K.; Pennycook, S. J.; Xie, J.

P.; Guan, C.; Wang, J. Open hollow Co-Pt clusters embedded in carbon nanoflake arrays for highly efficient alkaline water splitting. *J. Mater. Chem. A.* **2018,** 6, 20214-20223.

(9) Wang, J.; Zhong, H.-X.; Wang, Z.-L.; Meng, F.-L.; Zhang, X.-B. Integrated Three-Dimensional Carbon Paper/Carbon Tubes/Cobalt-Sulfide Sheets as an Efficient Electrode for Overall Water Splitting. *ACS Nano.* **2016,** 10, 2342-2348.

(10) Liang, Y. H.; Liu, Q.; Luo, Y. L.; Sun, X. P.; He, Y. Q.; Asiri, A. M. $Zn_{0.76}Co_{0.24}S/CoS_2$ nanowires array for efficient electrochemical splitting of water. *Electrochimica Acta.* **2016,** 190, 360-364.